Design and Development of Leo: An Affordable Biomechanically Inspired Quadruped Robot with Cognitive Abilities

Jubaer Tanjil Jami
Department of Mechanical Engineering
Bangladesh University of Engineering and Technology (BUET)
Dhaka, Bangladesh
jamijubaer@gmail.com

Taskin Mehereen
Department of Mechanical Engineering
Bangladesh University of Engineering and Technology (BUET)
Dhaka, Bangladesh
taskin2560@gmail.com

Munirul Alam
Department of Mechanical Engineering
Bangladesh University of Engineering and Technology (BUET)
Dhaka, Bangladesh
munirulalam15@gmail.com

Mir Tahmidur Rahman
Department of Mechanical Engineering
Bangladesh University of Engineering and Technology (BUET)
Dhaka, Bangladesh
mahirahman4258@gmail.com

***Abstract*—This paper presents the design, development, and testing of Leo, an affordable biomechanically inspired quadruped robot with cognitive abilities. The objective was to create an accessible, low-cost platform for robotics research and education. Leo features a lightweight 3D-printed structure weighing 2 kg, with dimensions of 550 mm x 400 mm x 100 mm. The robot employs a novel crankshaft mechanism in its leg design to reduce torque requirements and improve efficiency. Leo's control system integrates Robot Operating System (ROS) and Arduino, allowing for both manual and semi-autonomous operation. Cognitive abilities are demonstrated through voice recognition, image recognition, and object detection capabilities using YOLOv4 and face recognition algorithms. Gait analysis reveals an elliptical trajectory with each walking cycle lasting 19-20 seconds. Real-world testing showed a close correlation between planned and actual movements, with an approximate error of 25% due to practical conditions. Leo represents a significant step towards creating accessible quadruped robots for research, household use, and small-scale tasks, with potential applications in education, home assistance, and prototype testing for more advanced robotics systems.**

Keywords—Quadruped Robot, Biomechanics, Gait Analysis, ROS (Robot Operating System), Arduino, Object Detection (YOLOv4), Face Recognition, Voice Recognition, Affordability

I. INTRODUCTION

A large portion of indoor and outdoor land remains inaccessible to wheeled or tracked vehicles due to the presence of obstacles and uneven terrain. Legged robots, on the other hand, have the potential to navigate a wider variety of environments, making them a promising solution for these challenges. Hence, biomechanical legged robots are becoming increasingly prevalent in both research and commercial applications.[1][2]

Quadruped robots, in particular, have garnered significant attention due to their ability to traverse diverse terrains effectively. Quadruped locomotion systems can mimic not only static gaits of animals but also highly agile and dynamic behaviors, such as galloping, jumping, and spinning, which enable them to traverse unstructured terrains[2]. This is why quadruped robots find plenty of applications in the area of industrial applications [1], rough terrain navigation [3], military purposes[4], space exploration [5]and beyond [1].

A key consideration in quadruped robot design is the trade-off between material selection and overall weight. Lighter materials can enhance agility and reduce power consumption, while heavier materials offer robustness and can lead to increased power demands and potentially limit dynamic capabilities. The choice of materials often involves careful optimization based on the robot's intended applications and performance goals. [6]

Another important aspect of quadruped robot development is perception and environment interaction[7],[8]. Control systems of these robots vastly vary from manual to autonomous control, where machine learning algorithms may be used to impart image recognition abilities and voice recognition. Jin et al.[9] proposed a You Only Look Once (YOLO)-based perception module on quadruped robots to make them suitable for metro inspection. Sivacoumare et al. [10] introduced a low-cost, spider-like legged robot prototype controlled via a user-friendly speech interface, designed to assist the visually impaired with object detection and facial recognition tasks.

The locomotion mechanism of quadruped robots comprises of three primary motions to bring about the movement: supporting the body with a vertical bouncing motion, controlling the altitude of the body by using servo motors to impart hip torques during each leg's stance phase, and by placing the feet in key locations on each step with the help of principles of symmetry to keep the robots balanced as they moved about[11]. Although the details of the control have a machine-to-machine variation, they all share these three ingredients.

The gait algorithms for the motion of these robots to optimize stability and energy efficiency is an active area of research[2]. Collins et al. [12] explored the robustness and flexibility of a hard-wired central pattern generator (CPG) model in generating and transitioning between multiple quadrupedal gaits, illustrating its independence from specific oscillator dynamics or coupling schemes. Bellegarda et al. [13] integrated central pattern generators (CPGs), specifically

systems of coupled oscillators, into the deep reinforcement learning (DRL) framework to enable robust and omnidirectional quadruped locomotion.

Given the tremendous potential of quadruped robots, there has been considerable progress in this area in recent years. However, the high cost of manufacturing quadruped robots limits their accessibility and restricts their use and research opportunities. This paper introduces Leo, an open-source, low-cost quadruped robot platform with a focus on modularity, 3D-printability, and accessibility. Leo is a lightweight and affordable option for a quadruped robot that resembles the movement of a dog. With the ability to provide the locomotion capabilities of a normal quadruped robot, Leo is smaller, lighter, and has a much lower development cost than its more sophisticated counterparts, making it suitable for household use, research prototyping and testing, and other smaller scale tasks. Table I provides a comparative analysis of Leo against other existing quadruped robot platforms [14], [15], [16], [17]

In addition, Leo's voice and image recognition abilities make it a talking dog, allowing it to mimic the behavior of pet dogs that serve as dear companions to humans. The contributions of this paper are: (1) **Design and manufacture of the quadruped robot** Leo using light-weight and low-cost equipment (2) Semi-autonomous control using integration of voice and image recognition and elliptical trajectory for gait (3) Testing of the control mechanism and gait algorithm.

TABLE I. FEATURE COMPARISON OF THE ROBOT WITH THE EXISTING ROBOTS

Robot Name	**Legs**	**Mass[kg]**	**DoF**	**Cost[$]**	**Mode of control**
Leo	4	2	12	170	Manual/Semi-autonomous
Stanford Doggo[14]	4	4.8	8	3000	Manual
Minitaur[16]	4	5.0	8	N/A	Manual
Jerboa[15]	2	2.5	4	N/A	Manual
Mini Cheetah[17]	4	9	6	4,980	Manual

Fig. 1. Leo the quadruped robot

II. METHODOLOGY

A. *Mechanical Design*

The 3D modeling of Leo was completed using SolidWorks 2020. Leo is designed with a forward/backward configuration, reducing slippage between the feet and the ground, and improving motion performance. The dimensions are as follows: length 550 mm, width 400 mm, height 100 mm, and foot distance (front and rear) 350 mm. Leo features a symmetrical design with four identical legs, reducing development complexity and cost. The robot weighs 2 kg and the legs are 3D printed using polylactic acid (PLA).

The legs of the quadruped are in continuous contact with the ground, making their design crucial for successful locomotion. Bearings are used in the forward swing of the hip joint to carry axial forces. The thigh and lower leg were designed to minimize weight and inertia, reducing theoretical errors. The thigh has a dimension of 105 mm and the calf a dimension of 160 mm, as illustrated in Figure 2(a).

Instead of using a direct servo connection at the knee joint, a crankshaft mechanism is employed, where the lower leg is driven indirectly by a servo horn. This allows the servo to be placed on the upper side of the thigh near the hip joint, which experiences relatively low rotational inertia. Figure 2(b) illustrates the position of the motor.

If the servo motor is placed at the knee, the torque requirement increases compared to placing the servo motor at the upper part of the thigh. This is due to the greater distance between the axis of rotation in the first scenario. Understanding the torque needed for rotation is crucial in the design of robotic legs, and the analysis illustrated in Table II and equations (1) to (3). Figure 3 shows the torque requirements in both scenarios, proposing a crankshaft mechanism to lower the torque requirement.

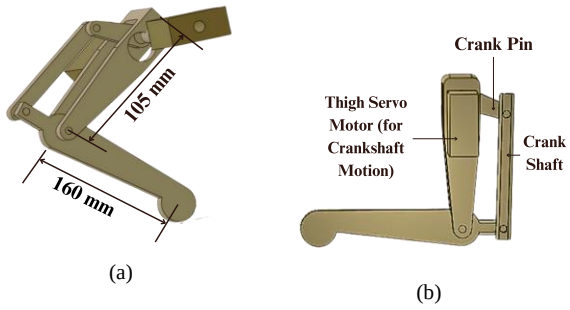

(a) (b)

Fig. 2. 3D model of the leg (a) thigh and calf dimensions (b) motor placement

TABLE II. QUANTITIES FOR TORQUE ANALYSIS

Symbol	**Quantity Specified**
T	Torque requirement to rotate the leg about its axis of rotation
W	Weight of the components in the leg
L	Distance between the axis of rotation of the leg and the weights acting on the leg due to various components in the first scenario
X	Distance between the axis of rotation of the leg and the weights acting on the leg due to various components in the second scenario

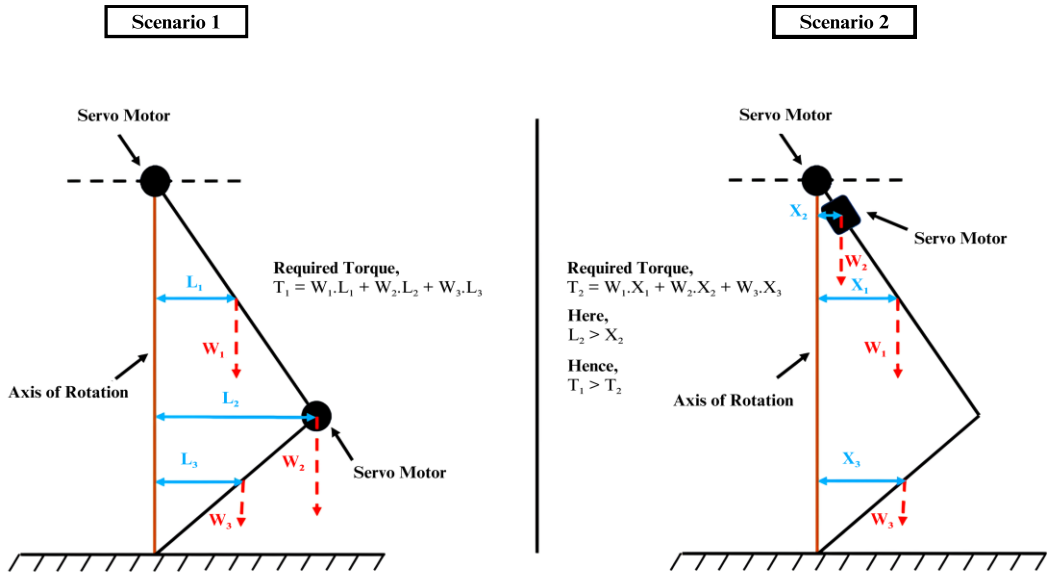

Fig. 3. Schematic diagram comparing torque requirements when the servo motor is placed at the knee (scenario 1) versus when it is placed at the thigh (scenario 2)

The total torque requirement in the first and second scenarios are given by (1) and (2) respectively

$$T_1 = W_1L_1 + W_2L_2 + W_3L_3 \quad (1)$$

$$T_2 = W_1X_1 + W_2X_2 + W_3X_3 \quad (2)$$

$$T_1 - T_2 = W_2(L_2 - X_2)$$

$$\therefore T_1 - T_2 > 0 \quad (3)$$

Since the quantity L_2 is larger than the quantity X_2, the torque requirement for the first scenario is larger as shown by (3). In the light of the above analysis, crank-shaft mechanism was used to lower the torque requirement.

The hip joint design, illustrated in Figure 4 provides two degrees of freedom—one for roll movement and one for pitch movement. Each movement is actuated by a separate servo, with the servo for the forward swing (pitch) motion mounted

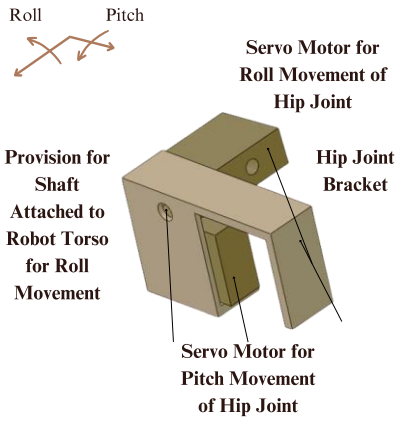

Fig. 4. 3D model of hip joint assembly

inside the hip-joint bracket to save space. The choice of actuator is critical for the locomotion performance of the quadruped robot. Due to the robot's weight, the actuator must generate high torque with a fast response and compact size. An MG996R servo is selected as the drive source. While the servo does not provide feedback for the angular displacement signal directly, its high built-in gear ratio makes it acceptable for low-speed gait and self-balancing tests.

The torso was cut to its desired shape using laser cutting of Poly Methyl Methacrylate (Acrylic Plastic) sheet. The overall structure of Leo has a total of twelve degrees of freedom and a full elbow leg arrangement. All four legs are identical in structure and size for ease of control. The hip joint is directly connected to the servo in two degrees of freedom (roll and pitch) to simplify the internal structure, while the knee joint is controlled by a crankshaft mechanism connected to a servo at the upper thigh to reduce the leg's inertia.

B. Software and Control Mechanism

The motion control is achieved through Robot Operating System (ROS) and Arduino interfacing, utilizing the gait algorithm developed. Upon startup, calibration of the twelve servo motors across four legs of Leo is performed to stand properly. To determine the 3D coordinates of each leg we used trigonometric calculations following an elliptical pathway to emulate the natural gait of a quadruped.

Leo operates on a Raspberry Pi 4 running ROS and can be controlled manually via Bluetooth or semi-autonomously. In manual mode, motion commands received over Bluetooth are processed by a gait algorithm that determines the leg angles necessary for standing, walking, and dancing. In the semi-autonomous mode, Leo uses both audio and image data to guide its movements. Audio is captured by an on-board microphone, noise is suppressed, and the audio is converted to text by the Vosk node for ROS. Specific instructions like “move forward” or “move backward” are extracted and

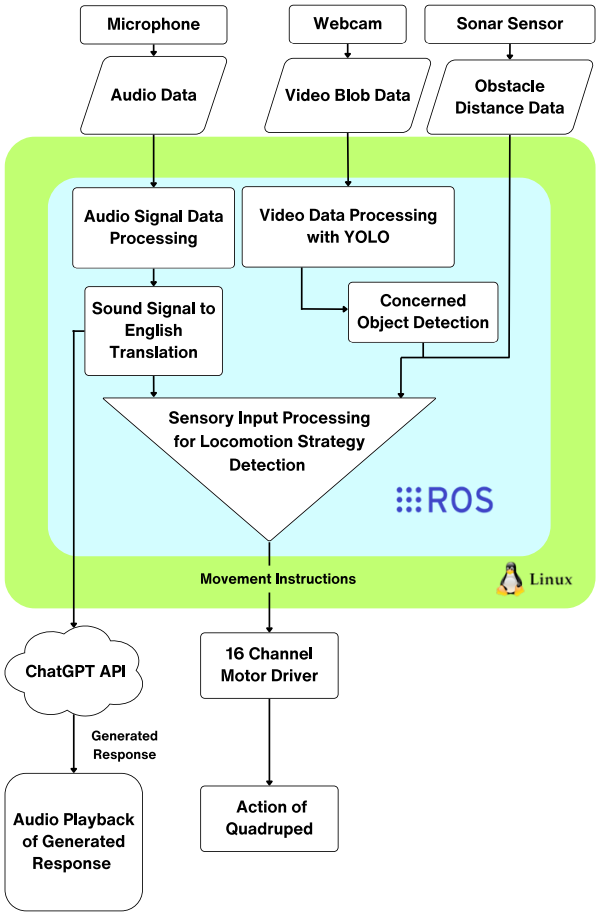

Fig. 5. System architecture of the semi-autonomous control mechanism of Leo

executed by Leo. Additionally, the text is sent to the Chat Generative Pre-Trained Transformer (ChatGPT) Application Programming Interface (API), allowing Leo to respond to virtually any query using a text-to-speech synthesizer, making it a capable companion bot. The communication system in Leo enables it to detect hazards and adjust its gait accordingly. To understand its surroundings, Leo utilizes YOLOv4 for common object detection, cutting-edge real-time object detection, and a face recognition system. These capabilities are applied to video data captured by a head-mounted camera, using the face-recognition Python package. The performance of these features is demonstrated in Figure 6, showcasing the test results for object detection and face recognition. The object detection system, combined with obstacle distance data from the sonar sensor, allow Leo to navigate its environment autonomously. Upon detecting a trained object, Leo signals the ROS node to activate the sonar sensor to collect distance data and stop movement if the distance exceeds a certain threshold. Face detection is used to identify the owner, enabling Leo to move towards them.

C. *Gait Analysis*

To determine the coordinates of each leg, we used trigonometric calculations following an elliptical pathway to emulate the natural gait of a quadruped, illustrated in Figure 7. The gait movement of Leo is controlled by the servo via instructions from the Arduino, manipulating the triangle formed by the torso and lower leg. This triangle consists of three lines: the thigh (BC, length q), the lower leg (CA, length

(a)

(b)

Fig. 6. View of Leo through head-mounted camera for (a) face detection and recognition (b) object detection

r), and the line between the lower leg tip that touches the ground and the torso tip connected to Leo's body (AB, length p). By controlling the length of AB, we achieved vertical movement, enabling Leo to stand. To perform walking motions, we formed an elliptical trajectory along tip A and controlled the angles between points B, C, and A. Equations (4) to (9) illustrate the trajectory of the motion taken by the torso and the leg as the quadruped completes a walking motion.

$$A' = cos^{-1}\frac{s^2 + r^2 - q^2}{2sr} \tag{4}$$

$$B' = cos^{-1}\frac{q^2 + s^2 - r^2}{2qs} \tag{5}$$

$$C' = cos^{-1}\frac{q^2 + r^2 - s^2}{2qr} \tag{6}$$

$$tan\,\theta = \frac{x}{p} \tag{7}$$

$$s = \frac{p}{cos\,\theta} \tag{8}$$

$$\frac{x^2}{q^2} + \frac{z^2}{r^2} = 1 \tag{9}$$

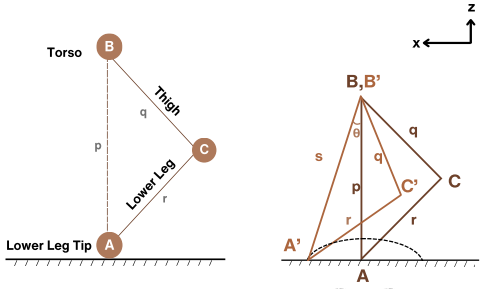

(a) (b)

Fig. 7. (a) Standing algorithm (b) Walking algorithm

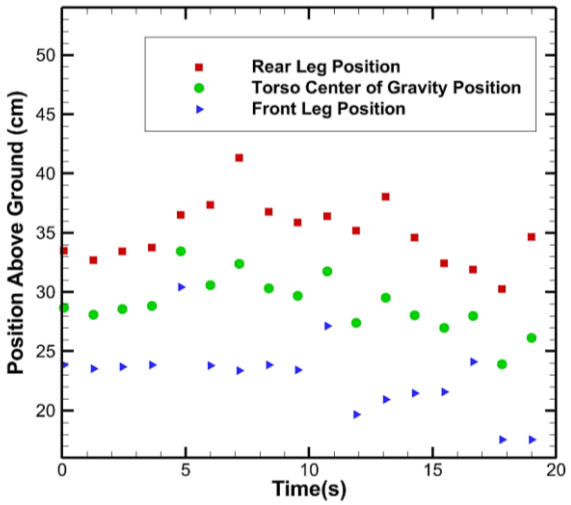

Fig. 8. Measured datapoints of variation of rear leg, torso center of gravity and front leg positions with time during one complete step

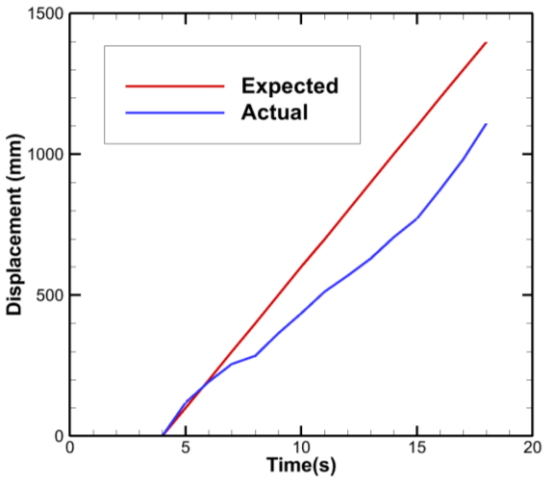

Fig. 10. Variation of expected versus actual displacement of Leo with time

LEO's motion was recorded using a 60 FPS camera. The frames were then extracted from the video. The resulting images were analyzed using ImageJ software and the leg length was measured. This provided sufficient data points to study the efficacy of the control algorithm, shown in Figure 8.

III. Results and Discussion

The study analyzed the positions of different parts of Leo—specifically, the rear leg, torso center of gravity, and front leg—over the course of one complete step. The results are depicted in Figure 9. It takes Leo approximately 7 seconds to reach its highest position, and each walking cycle lasts between 19 to 20 seconds. The elliptic shape of the fitted curve in the graph illustrates the elliptical trajectory derived from the gait algorithm, demonstrating the synchronization between the rear leg, torso center of gravity, and front leg during the walking motion.

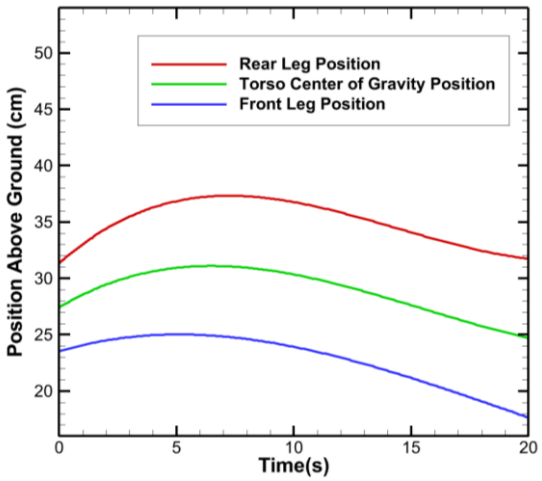

Fig. 9. Fitted curve of variation of rear leg, torso center of gravity and front leg positions with time during one complete step, denoting an elliptical trajectory

The YOLOv4 object detection model achieved an Average Precision (AP) of 43%. Additionally, the face detection package used for Leo provided a confidence score ranging from 40% to 60% for each detected face.

The comparison between Leo's expected and real displacement is shown in Figure 10. The graph reveals a close correlation between the planned and actual movements of Leo. The design aimed for Leo to achieve a displacement of 100 millimeters per cycle. However, real-world conditions cause slight deviations from the intended path over time, resulting in an approximate error of 25%. These deviations can be attributed to various losses that occur in practical scenarios compared to a perfectly controlled environment.

IV. Future Work

For future development, several improvements have been identified for Leo. For better reliability, a more rigid body material and metal servo gears should be used, as these components were unavailable during the initial development phase. The current velocity of Leo is insufficient for outdoor operations, so the gait control algorithm can be improved and optimized using Machine Learning and Deep Learning techniques to enhance performance. Although the current version of Leo is semi-autonomous, significant advancements can be made to achieve full autonomy by implementing features such as Simultaneous Localization and Mapping (SLAM). Additionally, the existing voice control features in Leo are hardcoded and can be made dynamic to improve user interaction. Leo currently cannot carry additional weights, and enhancing its load-carrying capability for industrial applications can be achieved through better gait and balancing algorithms. With further research, testing, and improvement, Leo has the potential to operate in hazardous environments where human presence is risky, such as industrial sites, military applications, fragile buildings, and polluted areas.

V. Conclusion

In conclusion, this work outlines Leo, an affordable biomechanically inspired quadruped robot, which has been successfully designed and developed with cognitive abilities. The following are the key contributions and findings from this work:

1) The robot features a lightweight, 3D-printed structure weighing 2 kg, with dimensions of 550 mm x 400 mm x 100 mm.

2) Leo employs a crankshaft mechanism in its leg design to reduce torque requirements and improve efficiency.

3) The robot's control system integrates ROS and Arduino, allowing for both manual and semi-autonomous operation.

4) Leo demonstrates cognitive abilities through voice recognition, image recognition, and object detection capabilities.

5) The gait analysis shows that Leo follows an elliptical trajectory, with each walking cycle lasting 19-20 seconds.

6) Real-world testing revealed a close correlation between planned and actual movements, with an approximate error of 25% due to practical conditions.

7) The YOLOv4 object detection model achieved an Average Precision of 43%, while the face detection package provided confidence scores of 40-60%.

Leo represents a significant step towards creating accessible, low-cost quadruped robots for research, household use, and small-scale tasks. Future improvements, such as using more rigid materials, optimizing gait control algorithms, and enhancing autonomy, could further expand Leo's capabilities and applications.

Acknowledgment

The authors would like to express their sincere gratitude to the esteemed course instructors: Mr. Mantaka Taimullah, Assistant Professor; Mr. Shahriar Alam, Lecturer; Mr. Priom Das, Lecturer; and Dr. Kazi Arafat Rahman, Professor, all from the Department of Mechanical Engineering at the Bangladesh University of Engineering and Technology. Their invaluable guidance was instrumental in the successful completion of this research, greatly enhancing the quality of this conference paper. The authors also extend their warm thanks to Mr. Shorup Chanda, Department of Mechanical Engineering, BUET, for his insightful support throughout the process. Additionally, the authors would also like to acknowledge Mr. Intesar Jawad Jaigirdar, Department of Computer Science, University at Buffalo for his valuable assistance in bringing this work to life.

References

[1] P. Biswal and P. K. Mohanty, 'Development of quadruped walking robots: A review', *Ain Shams Engineering Journal*, vol. 12, no. 2, pp. 2017–2031, Jun. 2021, doi: 10.1016/J.ASEJ.2020.11.005.

[2] H. Zhu *et al*., 'Terrain-Perception-Free Quadrupedal Spinning Locomotion on Versatile Terrains: Modeling, Analysis, and Experimental Validation', *Front Robot AI*, vol. 8, Oct. 2021, doi: 10.3389/frobt.2021.724138.

[3] M. Raibert, 'BigDog, the rough-terrain quadruped robot', in *IFAC Proceedings Volumes (IFAC-PapersOnline)*, 2008. doi: 10.3182/20080706-5-KR-1001.4278.

[4] J. Moses and G. Ford, 'See Spot save lives: fear, humanitarianism, and war in the development of robot quadrupeds', *Digital War*, vol. 2, no. 1–3, pp. 64–76, Dec. 2021, doi: 10.1057/s42984-021-00037-y.

[5] P. Arm *et al*., "SpaceBok: A Dynamic Legged Robot for Space Exploration," *2019 International Conference on Robotics and Automation (ICRA)*, Montreal, QC, Canada, 2019, pp. 6288-6294, doi: 10.1109/ICRA.2019.8794136.

[6] E. W. Hawkes and M. R. Cutkosky, 'Design of Materials and Mechanisms for Responsive Robots', *Annu. Rev. Control Robot. Auton. Syst. 2018*, vol. 1, pp. 359–84, 2018, doi: 10.1146/annurev-control-060117.

[7] J. He, J. Shao, G. Sun, and X. Shao, 'Survey of quadruped robots coping strategies in complex situations', *Electronics (Switzerland)*, vol. 8, no. 12. MDPI AG, Dec. 01, 2019. doi: 10.3390/electronics8121414.

[8] M. Xiangrui, S. Wang, C. Zhiqiang, and Z. Leijie, 'A Review of Quadruped Robots and Environment Perception'.

[9] X. Jin, X. Hou, S. Du, W. Liu, and S. Kong, 'A Vision Perception Module on Quadruped Robot in Metro Inspection', in *2022 6th International Conference on Automation, Control and Robots, ICACR 2022*, Institute of Electrical and Electronics Engineers Inc., 2022, pp. 12–16. doi: 10.1109/ICACR55854.2022.9935517.

[10] A. Sivacoumare, S. Sheethal Maria, S. Satheesh, T. Athul, V. Manikandan, and T. Vinopraba, 'AI Quadruped Robot Assistant for the Visually Impaired', in *IECON Proceedings (Industrial Electronics Conference)*, IEEE Computer Society, Oct. 2021. doi: 10.1109/IECON48115.2021.9589508.

[11] W. Saab and P. Ben-Tzvi, 'DESIGN AND ANALYSIS OF A ROBOTIC MODULAR LEG MECHANISM', 2016. [Online]. Available: http://www.asme.org/about-asme/terms-of-use

[12] J. J. Collins and S. A. Richmond, 'Biological cybemet Hard-wired central pattern generators for quadrupedal locomotion', 1994.

[13] G. Bellegarda and A. Ijspeert, 'CPG-RL: Learning Central Pattern Generators for Quadruped Locomotion', *IEEE Robot Autom Lett*, vol. 7, no. 4, pp. 12547–12554, Oct. 2022, doi: 10.1109/LRA.2022.3218167.

[14] N. Kau, A. Schultz, N. Ferrante and P. Slade, "Stanford Doggo: An Open-Source, Quasi-Direct-Drive Quadruped," *2019 International Conference on Robotics and Automation (ICRA)*, Montreal, QC, Canada, 2019, pp. 6309-6315, doi: 10.1109/ICRA.2019.8794436.

[15] T. Tsuda, H. Mochiyama and H. Fujimoto, "Robotic jerboa: A compact bipedal kick-and-slide robot powered by unidirectional impulse force generators," *2010 IEEE/RSJ International Conference on Intelligent Robots and Systems*, Taipei, Taiwan, 2010, pp. 2523-2524, doi: 10.1109/IROS.2010.5650286.

[16] D. J. Blackman, J. V. Nicholson, C. Ordonez, B. D. Miller, and J. E. Clark, 'Gait development on Minitaur, a direct drive quadrupedal robot', in *Unmanned Systems Technology XVIII*, SPIE, May 2016, p. 98370I. doi: 10.1117/12.2231105.

[17] S. H. Jeon, S. Kim and D. Kim, "Online Optimal Landing Control of the MIT Mini Cheetah," *2022 International Conference on Robotics and Automation (ICRA)*, Philadelphia, PA, USA, 2022, pp. 178-184, doi: 10.1109/ICRA46639.2022.9811796.